Available online at www.sciencedirect.com
ScienceDirect
Trans. Nonferrous Met. Soc. China 28(2018) 186−192
Transactions of Nonferrous Metals Society of China
www.tnmsc.cn

Leaching kinetics of selenium from copper anode slimes by nitric acid−sulfuric acid mixture

Hong-ying YANG, Xue-jiao LI, Lin-lin TONG, Zhe-nan JIN, Lu YIN, Guo-bao CHEN

School of Metallurgy, Northeastern University, Shenyang 110819, China

Received 20 September 2016; accepted 16 May 2017

Abstract: The leaching kinetics of selenium from copper anode slimes was studied in a nitric acid−sulfuric acid mixture. The effects of main parameters on selenium leaching showed that the leaching rate of selenium was practically independent of stirring speed, while dependent on temperature and the concentrations of HNO_3 and H_2SO_4. The leaching of selenium includes two stages. The activation energy in the first stage is 103.5 kJ/mol, and the chemical reaction is the rate controlling step. It was almost independent of H_2SO_4 concentration and dependent on HNO_3 concentration since the empirical reaction order with respect to HNO_3 concentration is 0.5613. In the second stage, the activation energy is 30.6 kJ/mol, and the process is controlled by a mixture of diffusion and chemical reaction. The leaching of selenium was almost independent of HNO_3 concentration.

Key words: selenium; kinetics; acid leaching; copper anode slimes

1 Introduction

Selenium, an essential element in advanced technologies, plays an important role in various fields, such as glass additive, solar cells and plain paper photocopies [1,2]. The independent deposit of selenium has been rarely found and 90% of selenium is extracted from copper anode slimes [2,3]. It has been reported that selenium presents mostly as intermetallic compounds containing silver, copper and selenides (Ag−Cu selenides) in the copper anode slimes [3−5].

Up to now, the approaches to recovering selenium from copper anode slimes include pyrometallurgical process [6,7] and hydrometallurgical process [8]. In the hydrometallurgical process, several agents have been employed, including sulfuric acid, sodium hydroxide, chlorine and chlorine-bearing oxidants [9]. 87% selenium can be extracted with 4 mol/L NaOH under atmospheric conditions [8] and 99% can be leached under pressure oxidation at a high temperature of 473.15 K [10]. Even so, it consumes more energy and needs alkali−acid conversion. Chlorine and chlorine-bearing oxidants can extract selenium efficiently, while the dispersal of Au and the product of poisonous chlorine cannot be avoided [11,12]. In sulfuric acid leaching process, the leaching efficiency is only 40%−50% even with high temperature and pressure [13]. To promote leaching efficiency, a new method with microwave assistance has been proposed by YANG et al [14], and hydrogen peroxide was added as oxidation agent. In that case, the high leaching efficiencies of 97.12% copper and 95.37% selenium were obtained, respectively. However, microwave is difficult to be applied in industry recently. Nitric acid, a strong oxidizing agent, which was used in INER process [9], can be added to sulfuric acid to improve the leaching efficiency of selenium. In previous work, leaching process with a nitric acid−sulfuric acid mixture has been proposed and selenium leaching can be divided into two stages. In the first stage, selenide is converted into elemental selenium (Reaction 1). In the second stage, the elemental selenium is converted to selenite (Reaction (2)) [15].

$$(Ag,\ Cu)Se+HNO_3 \rightarrow Cu^{2+}+Ag_2Se+Se+NO+H_2O \quad (1)$$

$$Se+HNO_3 \rightarrow SeO_3^{2-}+NO+H_2O \quad (2)$$

A remarkable extraction of selenium was successfully obtained. In this work, the leaching kinetics

Foundation item: Projects (51374066, U1608254) supported by the National Natural Science Foundation of China; Project (2014BAC03B07) supported by the National Key Technology R&D Program of China; Projects (2012223002, 2014020037) supported by Industrial Research Projects in Liaoning Province, China

Corresponding author: Hong-ying YANG; Tel: +86-24-83673932; E-mail: yanghy@smm.neu.edu.cn

DOI: 10.1016/S1003-6326(18)64652-7

of selenium from copper anode slimes in this acid mixture system has been investigated by determining parameters of the empirical reaction order and the apparent activation energy.

2 Experimental

2.1 Materials

The process mineralogy of the copper anode slimes has been investigated in our previous work [16,17]. The samples are similar to the ones with copper anode slimes bearing a high lead concentration [17]. The previous work indicated that 84% of the particle size is below 35 μm and its composition is complex. The main phases of the copper anode slimes include Au, Au−Pb alloys, eukairite, sulfate, arsenate, antimonite and oxygen. In the copper anode slimes, copper sulfate is the matrix that cements the finer particles together and selenium exists in the form of Ag−Cu selenide, which appears as spherical or ring-like shape. XRF analysis has been conducted on the copper anode slimes and the results are shown in Table 1. The main elements have been analyzed by inductively coupled plasma-atomic emission spectrometry (ICP−AES) and atomic absorption spectroscopy (AAS). The results are given in Table 2. All the reagents used in this investigation were analytical grade, and the water used was deionized water.

Table 1 XRF results of copper anode slimes (mass fraction, %)

SO_3	CuO	PbO	Ag_2O	CO_2	SeO_2	BaO
20.36	18.06	14.12	10.13	9.15	6.45	4.41
As_2O_3	Sb_2O_3	SiO_2	TeO_2	NiO	Cl	Bi_2O_3
4.06	3.60	2.16	1.59	1.54	1.08	0.94
Fe_2O_3	Al_2O_3	Cr_2O_3	Au	CaO	Co_2O_3	HfO_2
0.76	0.35	0.26	0.23	0.16	0.14	0.10
ZnO	PdO	SrO	K_2O	P_2O_5		
0.09	0.08	0.08	0.06	0.05		

Table 2 Chemical composition of main elements in copper anode slimes (mass fraction, %)

Au	Ag	Cu	Pb	Se	Ba
0.31	8.38	13.06	13.25	3.40	4.54

2.2 Procedure

The mixture of copper anode slimes (8 g) and acid (560 mL) composed of various concentrations of HNO_3 and H_2SO_4 was firstly given into a 1000 mL flask. Then, it was agitated at various temperatures in a water bath with various stirring speeds. During the experiments, 2 mL samples were withdrawn periodically from the reactor and analyzed by ICP-AES to determine the content of selenium. The leaching efficiencies (E) for selenium were calculated using the following equation:

$$E=10^{-4}C/(2w\rho) \quad (3)$$

where C (mass fraction, 10^{-6}) is the concentration of selenium in the filtrate diluted to 100 mL, w (%) is the mass fraction of selenium in the copper anode slimes, and ρ (g/mL) is the solid−liquid radio in the flask.

As silver can also be leached from copper anode slime during the leaching process, sodium chloride was added to the lixivium to precipitate silver after leaching.

3 Results and discussion

3.1 Results on leaching of selenium from copper anode slimes

3.1.1 Effect of temperature on selenium leaching

The influence of temperature on selenium leaching from copper anode slimes was investigated in temperature range of 353−368 K, under the following conditions: 0.5 mol/L HNO_3, 1.25 mol/L H_2SO_4 and stirring speed 300 r/min. The results are shown in Fig. 1.

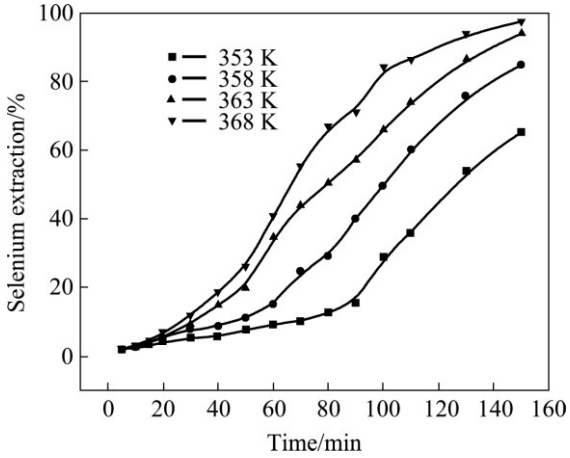

Fig. 1 Effect of temperature on selenium extraction (stirring speed: 300 r/min; HNO_3 concentration: 0.5 mol/L; H_2SO_4 concentration: 1.25 mol/L)

According to the slopes of curves in Fig. 1, selenium leaching curves can be divided into two stages. The slope value which can indicate the leaching rate of the process for the first stage is smaller and that for the second stage is larger. Temperature played an important role in the leaching rate. Time covered in the first stage decreased with the increase of leaching temperature. For example, at 353 K, the time covered in the first stage was 90 min, while it was 50 min at 368 K. At 353 K, 8.5% of selenium was leached in the first 90 min (the first stage) and the value increased to 65% in the following 60 min (the second stage). When the temperature increased to 368 K, 28.4% of selenium was leached in the first 50 min (the first stage) and the value increased to 97% in the following 100 min (the second stage).

3.1.2 Effect of stirring speed on selenium leaching

The effect of stirring speed on the extraction of selenium was studied in the range of 200−500 r/min. All experiments were carried out at the temperature of 358 K, an initial HNO_3 concentration of 0.5 mol/L and an initial H_2SO_4 concentration of 1.25 mol/L. As presented in Fig. 2, the leaching rates of selenium were almost independent of the stirring speed. It can be inferred that the reaction was mainly under chemical reaction control rather than diffusion control. Therefore, high stirring speed is not required and 300 r/min was chosen for further studies. With this stirring speed, solid particles were kept suspended in solution.

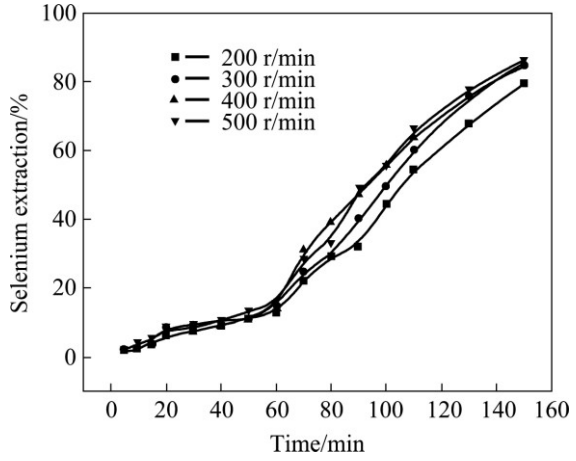

Fig. 2 Effect of stirring speed on selenium extraction (temperature: 358 K; HNO_3 concentration: 0.5 mol/L; H_2SO_4 concentration: 1.25 mol/L)

3.1.3 Effect of HNO_3 concentration on selenium leaching

Nitric acid, the main oxidizing agent for selenide, plays an important role in the leaching process [18]. The influence of the HNO_3 concentration ranging from 0.2 to 0.8 mol/L on the extraction of selenium was investigated when other conditions above were fixed. The results are shown in Fig. 3.

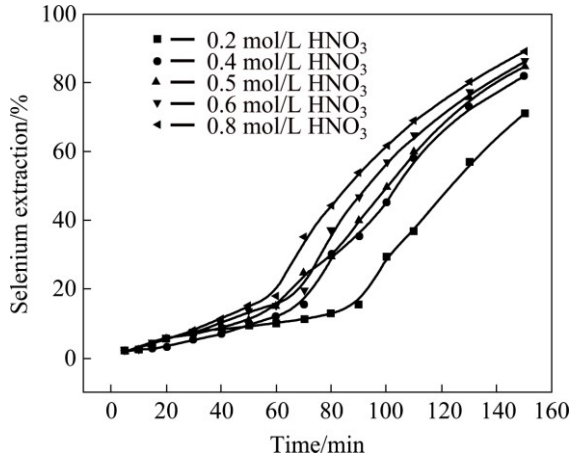

Fig. 3 Effect of HNO_3 concentration on selenium extraction (stirring speed: 300 r/min; temperature: 358 K; H_2SO_4 concentration: 1.25 mol/L)

It is clear that the leaching rate of selenium increased with the increase of HNO_3 concentration. The time covered for the first stage was shortened from 90 to 60 min when the HNO_3 concentration was increased from 0.2 to 0.8 mol/L. Meanwhile, after 150 min, 89% selenium was leached at 0.8 mol/L HNO_3, compared with 71% at 0.2 mol/L HNO_3.

3.1.4 Effect of H_2SO_4 concentration on selenium leaching

The influence of H_2SO_4 concentration ranging from 0.25 to 1.75 mol/L on the extraction of selenium was investigated with HNO_3 concentration of 0.5 mol/L and other conditions above were fixed. The results are shown in Fig. 4.

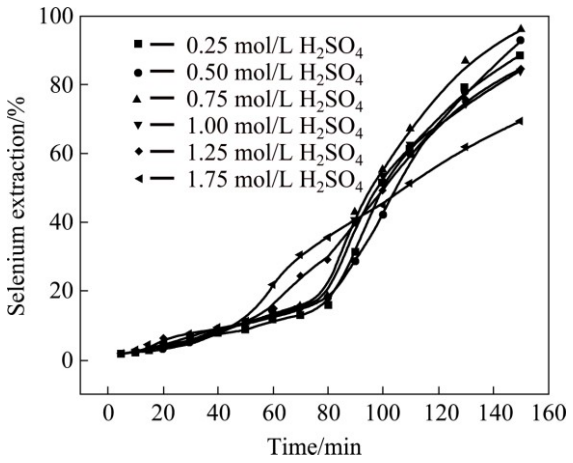

Fig. 4 Effect of H_2SO_4 concentration on selenium extraction (stirring speed: 300 r/min; temperature: 358 K; HNO_3 concentration: 0.5 mol/L)

According to Fig. 4, the influence of H_2SO_4 concentration on selenium leaching is very complex. In the first stage the leaching rate of selenium increased slightly with the increase of H_2SO_4 concentration. In the second stage, the leaching rate of selenium continued to increase slightly with the increase of H_2SO_4 concentration when its concentration was below 0.75 mol/L, whereas the value decreased with the increase when the H_2SO_4 concentration exceeded 0.75 mol/L. In the reaction, H_2SO_4 mainly acted as acid proton source [19]. Selenium leaching is affected by two factors: the oxidizing potential of NO_3^- ions and the potential for oxidation from selenide to elemental selenium (or selenite). The higher the former is, the easier the leaching rate of selenium is. The tendency of the later is on the contrary. When H_2SO_4 concentration increased, H^+ activity increased [19]. According to the φ−pH diagrams, both the oxidizing potential for NO_3^- ions and the potential for oxidation of selenide increased with the increase of solution acidity. When the H_2SO_4 concentration was below 0.75 mol/L, the variation value of the oxidizing potential of NO_3^- ions affected by H^+

activity may be larger than that of the potential for oxidation of selenide, which results in the slight increase of the leaching rate of selenium with the increase of H_2SO_4 concentration. The variable tendency of the potential is seemly inverse, resulting in the decrease of the leaching rate of selenium with further increase of H_2SO_4 concentration when it exceeds 0.75 mol/L. So, in this reaction, the critical H_2SO_4 concentration is 0.75 mol/L for a higher selenium leaching rate in this system.

3.2 Kinetic study on selenium leaching

The leaching process of selenium from copper anode slimes is a solid−liquid reaction. The shrinking core model is the most common kinetic model for this type of reaction. For this model, the reaction rate is generally controlled by diffusion through a liquid film, diffusion through a product layer, the chemical surface reaction or a mixed of diffusion and chemical reaction [19,20]. The integrated rate equation can be expressed as follows:

$$1-(1-x)^{1/3}=k_r t \text{ (chemical reaction controlled)} \quad (4)$$

$$1-(2/3)x-(1-x)^{2/3}=k_d t \text{ (diffusion controlled)} \quad (5)$$

where x is the fraction reacted, k_r is the chemical rate constant, k_d is the diffusion rate constant and t is the reaction time [21]. To determine the right kinetic model suitable for selenium leaching process, the experimental data shown in Fig. 1 were calculated based on Eqs. (4) and (5). The calculation was divided into two parts as there are two stages in the leaching process. The results are shown in Figs. 5(a) and (b), respectively. The dependency of these models on the kinetic data was evaluated using the correlation (R^2) and the results are shown in Table 3. It is clear that the experimental data fit better to the model of $1-(1-x)^{1/3}=k_r t$.

It is generally accepted that a chemically controlled process is strongly dependent on the temperature. The variation of the reaction rate with temperature is commonly described using the empirical Arrhenius law:

$$k=k_0\exp[-E_a/(RT)] \quad (6)$$

where k_0, E_a and R are the pre-exponential factor, the apparent activation energy and the mole gas constant, respectively [22].

According to the empirical Arrhenius law shown in Eq. (6), the plot of $\ln k$ versus $1000T^{-1}$ for two stages was constructed and the results are shown in Figs. 6 and 7 (the k values were determined from Fig. 5(a)). The slopes for the figures were $-E_a/R$. It was calculated that the activation energy for the first stage is 103.5 kJ/mol (>40 kJ/mol) and that for the second stage is 30.6 kJ/mol (between 12 kJ/mol and 40 kJ/mol) [23]. Obviously, the first stage is controlled by the surface chemical reaction and the second stage is controlled by a mixture of diffusion and chemical reaction.

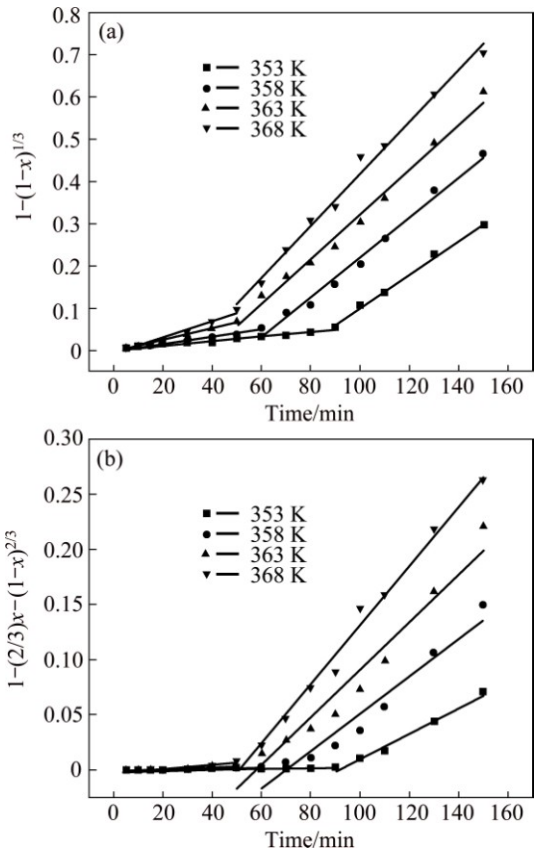

Fig. 5 Plots of data according to shrinking core model (stirring speed: 300 r/min; HNO_3 concentration: 0.5 mol/L; H_2SO_4 concentration: 1.25 mol/L): (a) $1-(1-x)^{1/3}$ versus time; (b) $1-(2/3)x-(1-x)^{2/3}$ versus time

Table 3 k_r, k_d values and correlation coefficients (R^2) for test temperatures

Stage	Temperature/K	k_r/(10^{-3} min^{-1})	R^2	k_d/(10^{-3} min^{-1})	R^2
First	353	0.5	0.9732	0.03	0.8556
	358	0.8	0.9729	0.04	0.8629
	363	1.5	0.9777	0.1	0.8613
	368	2.0	0.9629	0.2	0.8229
Second	353	4.0	0.996	1.15	0.9796
	358	4.8	0.9885	1.69	0.9311
	363	5.3	0.9898	2.16	0.9442
	368	6.2	0.9906	2.67	0.9874

To obtain the empirical reaction order with respect to the concentrations of sulfuric acid and nitric acid, the experimental data collected from Figs. 3 and 4 were analyzed based on Eq. (4) and the results are shown in Fig. 8−10, respectively. The k_r values and the correlations (R^2) of the two stages for the experiments are shown in Table 4.

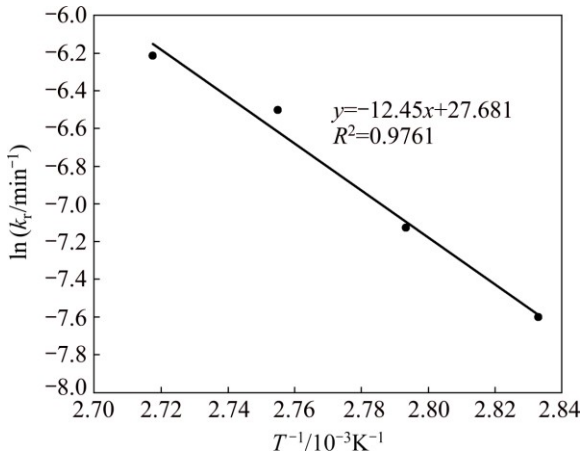

Fig. 6 Arrhenius plot for leaching of selenium (the first stage, values of k_r calculated from Fig. 5(a))

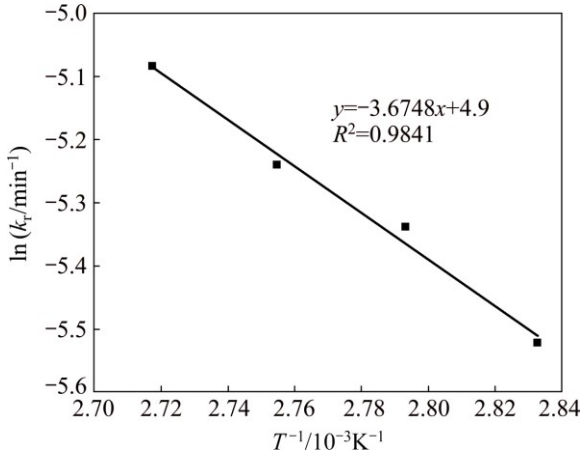

Fig. 7 Arrhenius plot for leaching of selenium (the second stage, values of k_r calculated from Fig. 5(a))

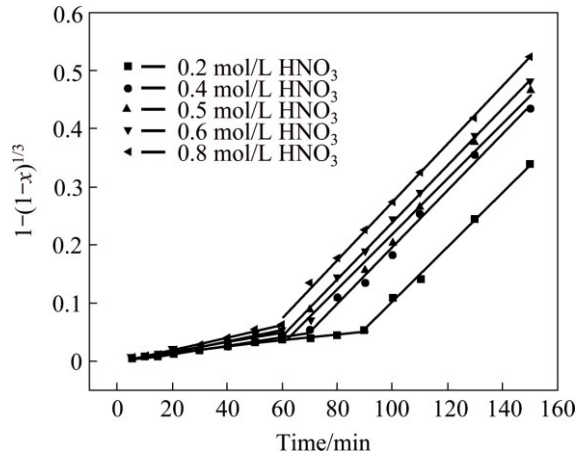

Fig. 8 Plots of $1-(1-x)^{1/3}$ versus time at different HNO_3 concentrations (stirring speed: 300 r/min; temperature: 358 K; H_2SO_4 concentration: 1.25 mol/L)

Figure 11 presents the plot of $\ln k_r$ versus $\ln c_{HNO_3}$ for the first stage. The reaction order can be determined from the slope. The calculation gives the empirical reaction order for the concentration of HNO_3 and the

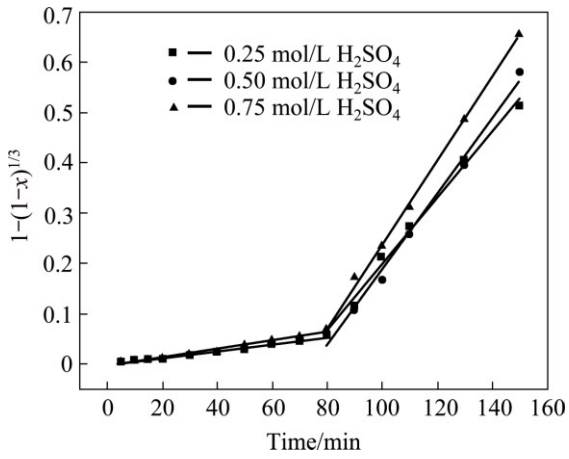

Fig. 9 Plots of $1-(1-x)^{1/3}$ versus time at different H_2SO_4 concentrations (≤0.75 mol/L) (stirring speed: 300 r/min; temperature: 358 K; HNO_3 concentration: 0.5 mol/L)

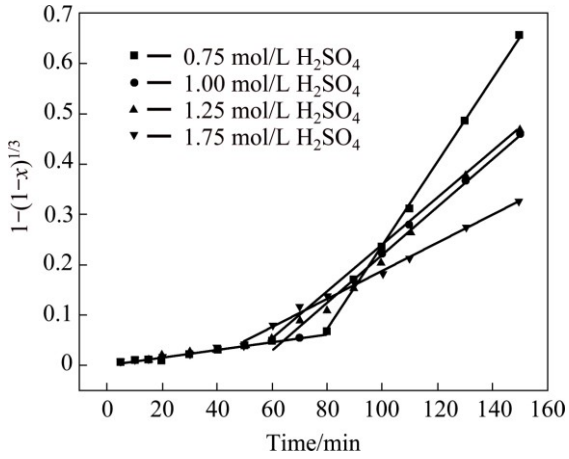

Fig. 10 Plots of $1-(1-x)^{1/3}$ versus time at different H_2SO_4 (≥0.75 mol/L) concentrations (stirring speed: 300 r/min; temperature: 358 K; HNO_3 concentration: 0.5 mol/L)

Table 4 Reaction rates (k_r) and correlations (R^2) for experimental data

Acid	concentration/ (mol·L^{-1})	The first stage		The second stage	
		k_r/ (10^{-3} min^{-1})	R^2	k_r/ (10^{-3} min^{-1})	R^2
HNO_3	0.2	0.5	0.982	4.7	0.9970
	0.4	0.7	0.9689	4.8	0.9932
	0.5	0.8	0.9729	4.8	0.9885
	0.6	0.9	0.9859	4.9	0.9944
	0.8	1.1	0.9907	5.0	0.9984
H_2SO_4	0.25	0.7	0.9841	6.6	0.9938
	0.50	0.8	0.9885	7.5	0.9916
	0.75	0.8	0.9855	8.3	0.9983
	1.00	0.8	0.9893	5.4	0.9785
	1.25	0.8	0.9729	4.8	0.9885
	1.75	0.7	0.9947	2.8	0.9957

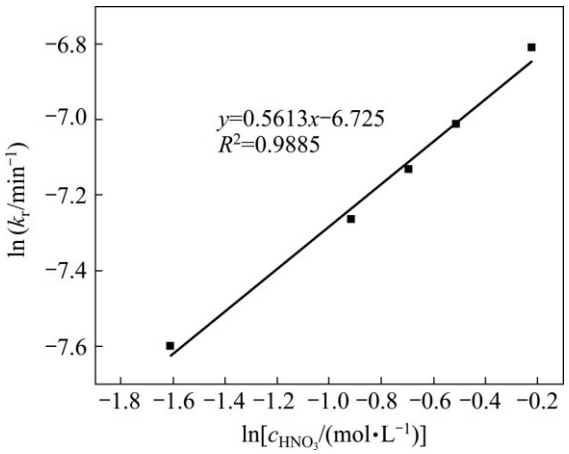

Fig. 11 Plot of $\ln k_r$ versus $\ln c_{HNO_3}$ (the first stage, values of k calculated from Fig. 8)

value is 0.5613. For the second stage, the k_r values are similar, which indicate that the effect of HNO_3 is slight.

With increasing H_2SO_4 concentration, the k_r values for the first stage almost remained the same. However, for the second stage the k_r values increased slightly when the concentration of H_2SO_4 was below 0.75 mol/L, while it decreased apparently when the H_2SO_4 concentration was above 0.75 mol/L. Figure 12 shows the plot of $\ln k_r$ versus $\ln c_{H_2SO_4}$ for the second stage. The orders of the reactions with respect to the concentration of H_2SO_4 are found to be 0.206 (<0.75 mol/L) and −1.2351 (≥0.75 mol/L). So, H_2SO_4 has a negative effect on the selenium leaching at a higher concentration.

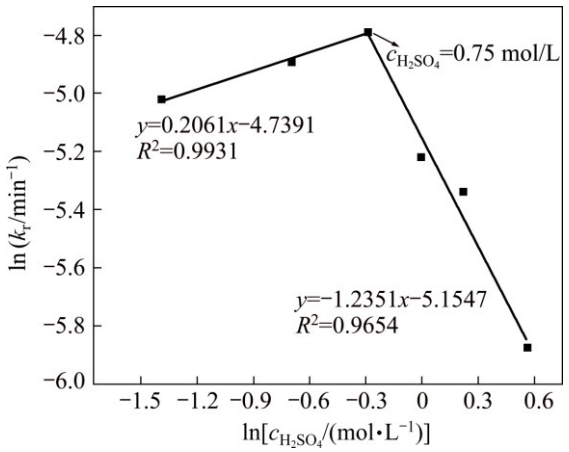

Fig. 12 Plots of $\ln k_r$ versus $\ln c_{H_2SO_4}$ (the second stage, values of k calculated from Figs. 9 and 10)

4 Conclusions

1) The leaching rate of selenium was practically independent of stirring speed, while dependent on temperature and the concentrations of HNO_3 and H_2SO_4. The leaching process of selenium includes two stages and the kinetic data for both the stages show good fit to the chemical control model.

2) For the first stage, the activation energy is 103.5 kJ/mol, which indicates that the first stage is controlled by the surface chemical reaction. The leaching of selenium in the first stage is almost independent of H_2SO_4 concentration and the empirical reaction order with respect to HNO_3 concentration is 0.5613.

3) For the second stage, the activation energy is 30.6 kJ/mol, which indicates that the second stage is controlled by a mixture of diffusion and chemical reaction. The leaching of selenium is almost independent of HNO_3 concentration. As to the H_2SO_4 contration, the empirical reaction order is 0.206 when the concentration of H_2SO_4 is below 0.75 mol/L. However, when the concentration is above 0.75 mol/L, the empirical reaction order is −1.2351.

References

[1] SPINKS S C, PARNELL J, BELLIS D, STILL J. Remobilization and mineralization of selenium–tellurium in metamorphosed red beds: Evidence from the Munster Basin, Ireland [J]. Ore Geology Reviews, 2016, 72: 114−127.

[2] MOSS R L, TZIMAS E, KARA H, WILLIS P, KOOROSHY J. Critical metals in strategic energy technologies: Assessing rare metals as supply-chain bottlenecks in low-carbon energy technologies [R]. Institute for Energy and Transport IET. 2011: 141−143.

[3] SCOTT J D. Electrometallurgy of copper refinery anode slimes [J]. Metallurgical & Materials Transactions B, 1990, 21(4): 629−635.

[4] TASKINEN P, PATANA S, KOBYLIN P, LATOSTENMAA P. Oxidation mechanism of silver selenide [J]. Oxidation of Metals, 2013, 81(5−6): 503−513.

[5] CHEN T T, DUTRIZAC J E. Mineralogical characterization of anode slimes—II. Raw anode slimes from Inco's copper cliff copper refinery [J]. Canadian Metallurgical Quarterly, 1988, 27(2): 97−105.

[6] TASKINEN P, PATANA S, KOBYLIN P, LATOSTENMAA P. Roasting selenium from copper refinery anode slimes [C]//Copper Metallurgy. Krakow, Poland, 2011: 1−8.

[7] LU Dian-kun, CHANG Yong-feng, YANG Hong-ying, XIE Feng. Sequential removal of selenium and tellurium from copper anode slime with high nickel content [J]. Transactions of Nonferrous Metals Society of China, 2015, 25(4): 1307−1314.

[8] KILIC Y, KARTAL G, TIMUR S. An investigation of copper and selenium recovery from copper anode slimes [J]. International Journal of Mineral Processing, 2013, 124: 75−82.

[9] HAIT J. Processing of copper electrorefining anode slime: A review [J]. Mineral Processing & Extractive Metallurgy C, 2009, 118(4): 240−252.

[10] LIU W F, YANG T Z, ZHANG D C, CHEN L, LIU Y N. Pretreatment of copper anode slime with alkaline pressure oxidative leaching [J]. International Journal of Mineral Processing, 2014, 128(5): 48−54.

[11] HAIT J, JANA R K, KUMAR V, SANYAL S K. Some studies on sulfuric acid leaching of anode slime with additives [J]. Industrial & Engineering Chemistry Research, 2002, 41(25): 6593−6599.

[12] HAIT J, JANA R K, SANYAL S K. Mineralogical characteristics of copper electrorefining anode slime and its leached residues [J]. Industrial & Engineering Chemistry Research, 2004, 43(9): 2079−2087.

[13] ZHANG Bo-ya, WANG Ji-kun. The technological research on

pre-treating copper anode slime with pressure acid leaching method [J]. Mining and Metallurgical Engineering, 2007, 27(5): 41−43. (in Chinese)

[14] YANG Hong-ying, MA Zhi-yuan, HUANG Song-tao, LV Yang, XIONG Liu. Intensification of pretreatment and pressure leaching of copper anode slime by microwave radiation [J]. Journal of Central South University, 2015, 22(12): 4536−4544.

[15] MOKMELI M, WASSINK B, DREISINGER D. Kinetics study of selenium removal from copper sulfate–sulfuric acid solution [J]. Hydrometallurgy, 2013, 139: 13−25.

[16] LI Xue-jiao, YANG Hong-ying, TONG Lin-lin, CHEN Guo-bao. Technological mineralogy of copper anode slime [J]. Journal of Northeastern University: Natural Science, 2013, 34(4): 560−563. (in Chinese)

[17] YANG Hong-ying, LI Xue-jiao, TONG Lin-lin, CHEN Guo-bao. Process mineralogy of high lead copper anode slime [J]. The Chinese Journal of Nonferrous Metals, 2014, 24(1): 269−278. (in Chinese)

[18] XIE Y, XU Y, YAN L, YANG R. Recovery of nickel, copper and cobalt from low-grade Ni−Cu sulfide tailings [J]. Hydrometallurgy, 2005, 80(1−2): 54−58.

[19] GHARABAGHI M, IRANNAJAD M, AZADMEHR A R. Leaching kinetics of nickel extraction from hazardous waste by sulphuric acid and optimization dissolution conditions [J]. Chemical Engineering Research and Design, 2013, 91(2): 325−331.

[20] CHEN T T, DUTRIZAC J E. A Mineralogical study of the deportment and reaction of silver during copper electrorefining [J]. Ecological Entomology, 2012, 37(1): 56−64.

[21] GHARABAGHI M, IRANNAJAD M, NOAPARAST M. A review of the beneficiation of calcareous phosphate ores using organic acid leaching [J]. Hydrometallurgy, 2010, 103(1−4): 96−107.

[22] ZHANG W, LI J, ZHAO Z. Leaching kinetics of scheelite with nitric acid and phosphoric acid [J]. International Journal of Refractory Metals and Hard Materials, 2015, 52: 78−84.

[23] AWE S A, SAMUELSSON C, SANDSTR M Å. Dissolution kinetics of tetrahedrite mineral in alkaline sulphide media [J]. Hydrometallurgy, 2010, 103(1−4): 167−172.

硝/硫混酸浸出铜阳极泥中硒的动力学

杨洪英，李雪娇，佟琳琳，金哲男，殷 璐，陈国宝

东北大学 冶金学院，沈阳 110819

摘 要：研究在硝/硫混酸体系中浸出铜阳极泥中硒的动力学和影响硒的浸出过程的主要参数。结果表明，硒的浸出速率与搅拌速度无关，而与浸出温度以及硫酸和硝酸的浓度相关。硒的浸出包括两个阶段：在第一阶段，硒的浸出活化能为 103.5 kJ/mol，硒的浸出主要由化学反应控制，硒的浸出与硫酸浓度无关，而与硝酸浓度相关，其反应级数为 0.5613；在第二阶段，硒的浸出活化能为 30.6 kJ/mol，硒的浸出由扩散和化学反应混合控制。此时，硒的浸出与硝酸的浓度基本无关。

关键词：硒；动力学；酸浸；铜阳极泥

(Edited by Wei-ping CHEN)